BJR

Received: 3 August 2015 | Revised: 22 September 2015 | Accepted: 7 October 2015

doi: 10.1259/bjr.20150646

Cite this article as:
Xu X-Q, Su G-Y, Liu J, Hu H, Hong X-N, Shi H-B, et al. Intravoxel incoherent motion MR imaging measurements of the bilateral parotid glands at 3.0-T MR: effect of age, gender and laterality in healthy adults. *Br J Radiol* 2015; **88**: 20150646.

FULL PAPER

Intravoxel incoherent motion MR imaging measurements of the bilateral parotid glands at 3.0-T MR: effect of age, gender and laterality in healthy adults

XIAO-QUAN XU, MD, GUO-YI SU, MD, JUN LIU, MD, HAO HU, MD, XUN-NING HONG, MD, PhD, HAI-BIN SHI, MD, PhD and FEI-YUN WU, MD, PhD

Department of Radiology, The First Affiliated Hospital of Nanjing Medical University, Nanjing, China

Address correspondence to: Dr Fei-Yun Wu
E-mail: *wfy_njmu@163.com*

Xiao-Quan Xu and Guo-Yi Su contributed equally to this manuscript.

Objective: To investigate the effect of age, gender and laterality on the intravoxel incoherent motion (IVIM) MR imaging measurements of parotid glands in healthy participants at 3.0-T MRI.
Methods: A total of 108 healthy participants were prospectively recruited. IVIM MRI scan was performed using a 3.0-T MR scanner, and corresponding parameters (perfusion fraction, *f*; pseudodiffusion coefficient, *D**; tissue diffusivity, *D*) were derived from biexponential fitting of IVIM data. Pearson correlation analysis was performed to determine the association between the IVIM MRI parameters and age. The parameter difference between male and female participants or between left and right parotid glands was compared using unpaired or paired *t* test, respectively.
Results: Excellent interreader and intrareader agreements on the measurements of IVIM MRI parameters were achieved. Both *D* and *f* values correlated inversely with the age in both left and right parotid glands ($p < 0.05$) while *D** value did not ($p > 0.05$). Male participants had higher IVIM MRI parameters than the female participants in both left and right glands ($p < 0.05$). No significant differences were found in the IVIM MRI parameters between left and right glands in both male and female participants ($p > 0.05$).
Conclusion: The IVIM MRI parameters are age and gender dependent, but not laterality dependent. Age- and gender-related effect should be taken into consideration in future IVIM MRI studies for parotid glands.
Advances in knowledge: (1) Both *D* and *f* values correlated inversely with the age in healthy parotid glands, while *D** value did not. (2) The parotid glands of males showed higher IVIM MRI parameters than that of females. (3) There were no significant differences on the IVIM MRI parameters between the left and right glands. (4) Age- and gender-related effect should be taken into consideration in future IVIM MRI studies for parotid glands.

INTRODUCTION

CT and MRI play an important role in the diagnosis and evaluation of parotid gland disease.[1–3] Previous studies[4,5] have demonstrated that some simple imaging-related quantitative measurement of the parotid gland, such as the gland volume, CT values and T_1 weighted signal intensity, correlated well with the pathophysiological process of some parotid gland disease. However, several other articles[6–8] also have proposed that some individual differences, such as the age and gender, could have an effect on the quantitative imaging-related measurement of the parotid gland. Therefore, such individual differences must be taken into consideration during the quantitative imaging studies of the parotid gland.

Recently, intravoxel incoherent motion (IVIM) MRI, which can simultaneously assess both the diffusion and perfusion characteristics of the tissue without the need of contrast material, has attracted more and more attention.[9,10] Encouraging results that use the IVIM MRI model have been acquired in various pathologies of the parotid gland, including the differentiation of benign and malignant tumours and evaluation of radiation-induced changes.[11–13] Nevertheless, studies validating the influence of some individual differences, such as the age and gender, on the IVIM MRI measurement of parotid gland were lacking until now.

Therefore, the purpose of this study was to investigate the effect of age, gender and laterality on the IVIM MRI measurement of parotid glands in healthy participants at 3.0-T MRI.

METHODS AND MATERIALS

Study population

This study was approved by the ethics committee of The First Affiliated Hospital of Nanjing Medical University, and written informed consent was obtained from all the healthy participants recruited. All participants were selected among persons who underwent health screening of the brain in our hospital from July 2014 to August 2015. IVIM MRI of the parotid gland was added into the routine MR protocol of brain MR examination during that period. Fasting and water deprivation were required at least 6 h before MR examination.

Conventional MRI results, clinical history and recent laboratory results were reviewed. We enrolled the participants based on the following inclusion criteria: (1) age more than 18 years, with body mass indices <25; (2) non-smokers and not addicted to alcohol; (3) not taking any medication at the time of imaging examination; (4) no known medical history of parotid gland disease, such as tumour, Sjögren's syndrome etc.; (5) no parotid gland abnormality observed on conventional MRI; (6) adequate image quality without significant susceptibility artefacts. Finally, 108 healthy participants (mean age, 40.2 ± 15.3 years; age range, 23–77 years) were included in our study. The 108 participants included 72 female (mean age, 41.8 ± 13.9 years; age range, 23–74 years) and 36 male (mean age, 37.0 ± 17.6 years; age range, 23–77 years) participants.

Imaging protocol

MRI examinations were performed by using a 3.0-T clinical MR (Verio Tim; Siemens Healthcare, Erlangen, Germany) and a 12-channel head coil. The conventional MRI protocol of the parotid gland included: (1) unenhanced axial T_1 weighted imaging [repetition time (TR)/echo time (TE), 900/10 ms; section thickness, 4 mm; intersection gap, 1.0 mm; field of view, 18 cm; and matrix, 384 × 336]; (2) axial T_2 weighted imaging (TR/TE 5000/99 ms; section thickness, 4 mm; intersection gap, 1.0 mm; field of view, 18 cm; and matrix, 384 × 336) with fat saturation; (3) coronal T_2 weighted imaging (TR/TE 5000/100 ms; section thickness, 4 mm; intersection gap, 1.0 mm; field of view, 22 cm; and matrix, 384 × 336) with fat saturation.

IVIM MRI was performed using single-shot echoplanar imaging. Detailed imaging parameters were TR/TE, 5000/74 ms; section thickness, 5 mm; intersection gap, 0.5 mm; field of view,

Figure 1. Conventional axial T_1 weighted (a) and T_2 weighted images (b), an example of region of interest selection (c) and the corresponding parametric maps (d–f) derived from intravoxel incoherent motion (IVIM) MRI in a 48-year-old female participant. The IVIM-derived parameters of the bilateral parotid glands in this patient were: left parotid gland: D, 0.9682×10^{-3} mm^2 s^{-1}; D^*, 20.7003×10^{-3} mm^2 s^{-1}; f, 0.2091; right parotid gland: D, 0.9854×10^{-3} mm^2 s^{-1}; D^*, 21.1071×10^{-3} mm^2 s^{-1}; f, 0.2083.

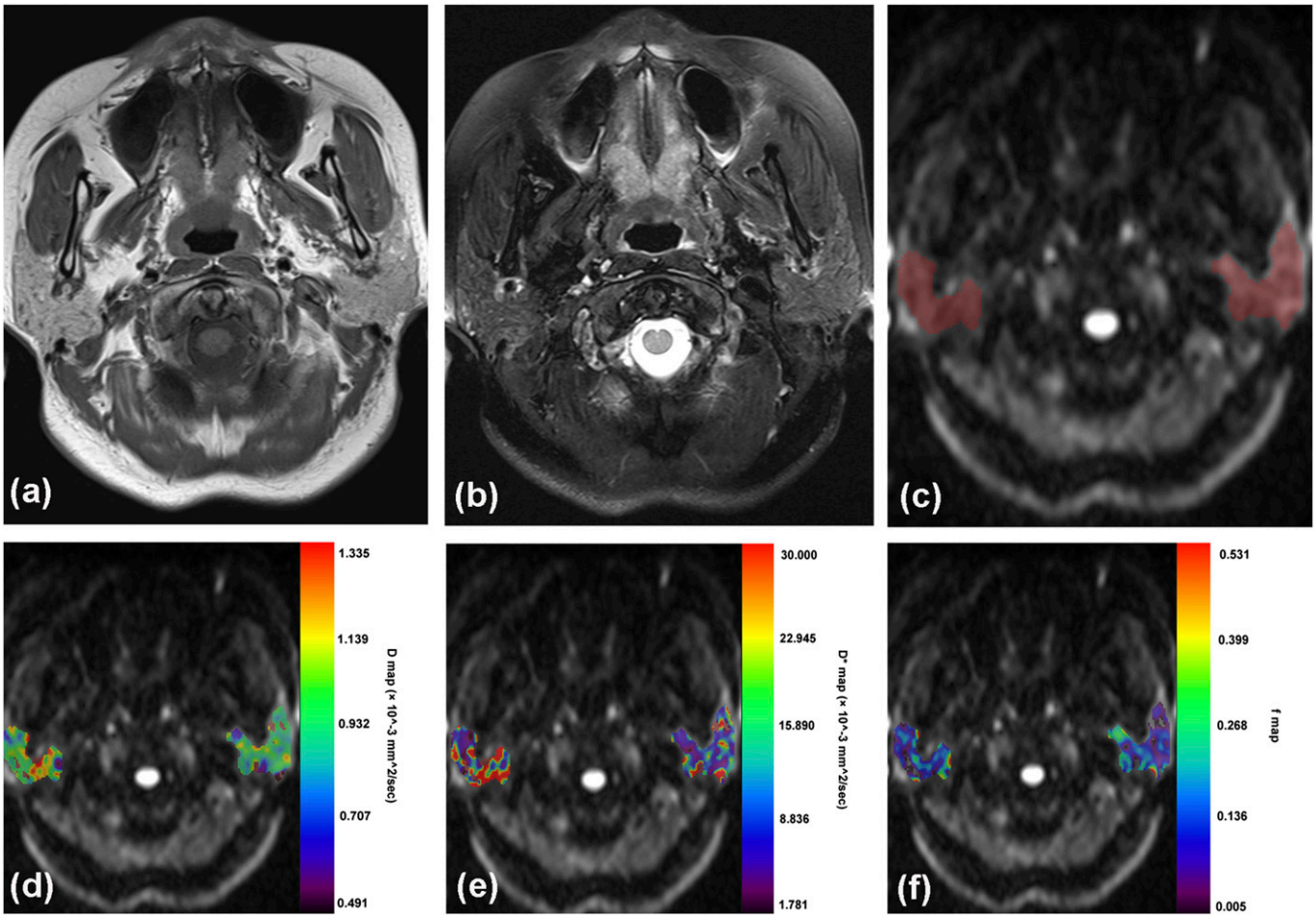

22 cm; and matrix, 130 × 100; parallel imaging factor, two. We acquired nine different *b*-values (0, 50, 100, 150, 200, 400, 600, 800 and 1000 s mm^{-2}) in three orthogonal directions for IVIM MRI scan. The total acquisition time was 4 min 55 s.

Intravoxel incoherent motion fitting

The relationship between signal variation and *b*-values in an IVIM-type sequence can be expressed by the following equation:[14]

$$S_b/S_0 = (1-f)e^{-bD} + fe^{-bD*}$$

where S is the mean signal intensity, S_0 is the signal intensity without diffusion, S_b is the mean signal intensity with a gradient sensitivity factor b. f describes the fraction of incoherent signal that arises from the vascular compartment in each voxel over the total incoherent signal. D is the diffusion parameter representing true molecular diffusion, and D^* is the pseudodiffusion coefficient, which describes macroscopic incoherent movement of blood in the microvasculature compartment.

To obtain the IVIM parameters, the above-mentioned IVIM signal equation was fitted in two steps.[15] In the first step, the curve was fitted for *b*-values >200 s mm^{-2} for the single parameter D. This assumes that D^* is significantly greater than D, so that the influence of pseudodiffusion on signal decay can be neglected for *b*-values >200 s mm^{-2}. In the second step, keeping the D value acquired in the first step constant, the curve was fitted for f and D^* over all *b*-values. This two-step method was used to increase robustness under biological conditions.

Image processing

All IVIM MRI data were transferred in digital imaging and communications in medicine format from the MRI scanner to an independent personal computer and processed using an in-house program with MATLAB® software (MathWorks® Inc., Natick, MA). The regions of interest (ROIs) were drawn on all imaging sections encompassing as much of the parotid gland area, while visually surrounding blood vessels were excluded with reference to the T_2 weighted images. The ROIs were slightly smaller in size than the actual size of parotid gland to reduce the influence of partial volume effect. The IVIM MRI measurements obtained from each ROI were averaged.

A total of three independent IVIM MRI measurements were performed in each participants by two readers, who had 14 (Reader 1, FYW) and 4 (Reader 2, XQX) years' clinical experience in head and neck radiology and were blinded to all demographic information. The measurements of the two radiologists were used to calculate interreader agreement. To assess the intrareader agreement, the second reader reassessed all the images, which were presented in a different order, 1 month after the first-time assessment. The average of the two measurement results of the second reader was employed into statistical analysis.

Statistical analysis

All continuous data were presented as the mean and standard deviation. Normality of the IVIM MRI parameters was analysed with Kolmogorov–Smirnov test. Pearson correlation analysis was performed to determine the associations between the IVIM MRI parameters and age. The paired *t* test was performed to compare the difference on IVIM parameters between left and right

Figure 2. Scatter plots of age effects on the measurements of D, f and D^* values in bilateral parotid glands. Correlation analyses indicated that there were significant inverse correlations between age and D or f values in both left (D, $p < 0.0001$, $r = -0.5035$; f, $p < 0.0001$, $r = -0.5265$) and right (D, $p < 0.0001$, $r = -0.5700$; f, $p < 0.0001$, $r = -0.5690$) parotid glands, while no significant correlation was found between age and D^* values in both left (D^*, $p = 0.0688$, $r = -0.1758$) and right (D, $p = 0.1209$, $r = -0.1503$) parotid glands.

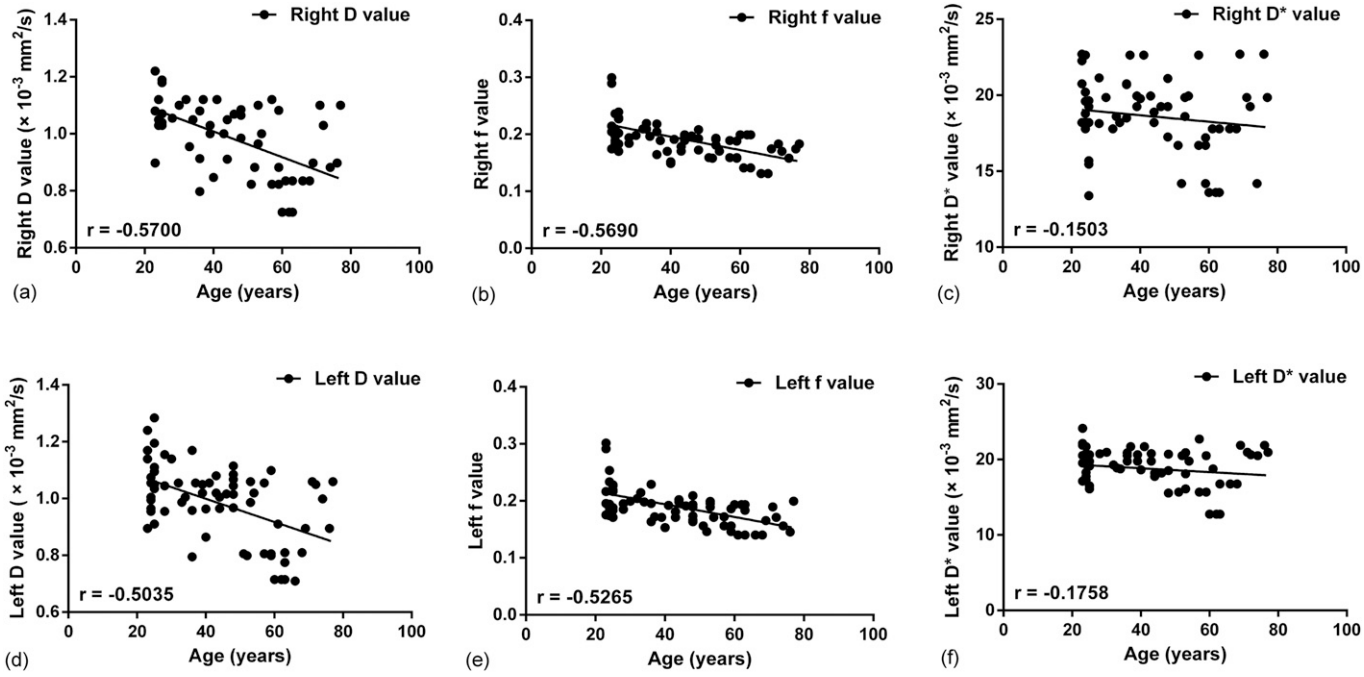

Table 1. Effect of gender on the intravoxel incoherent motion MRI parameters of bilateral parotid glands

Parameter	Left			Right		
	D	*D**	*f*	*D*	*D**	*f*
Female	0.9749 ± 0.1295	18.0044 ± 2.0851	0.1896 ± 0.0267	0.9819 ± 0.1262	17.8671 ± 2.0236	0.1908 ± 0.0269
Male	1.0492 ± 0.0970	20.5543 ± 1.3862	0.2051 ± 0.0423	1.0636 ± 0.0939	20.3660 ± 1.4198	0.2079 ± 0.0399
p-value	0.0041	<0.0001	0.0468	0.0014	<0.0001	0.0208

*D**, pseudodiffusion coefficient; *D*, tissue diffusivity; *f*, perfusion fraction.
Except *p*-values, data are expressed as mean ± standard deviation. The unit for *D* and *D** value is $\times 10^{-3}\,mm^2\,s^{-1}$.

parotid glands. The unpaired *t* test was performed to compare the difference on IVIM parameters between male and female healthy participants.

Interreader and intrareader agreement on the IVIM MRI measurements was assessed by using the intraclass correlation coefficient (ICC) with 95% confidence intervals. The ICC ranged between 0 and 1.00, and the values closer to 1.00 meant better reproducibility. They were interpreted as follows: $r < 0.40$, poor; $r = 0.41$–0.60, moderate; $r = 0.61$–0.80, good; $r \geq 0.81$, excellent. A two-side *p*-value <0.05 indicated statistical significance. Statistical analyses were performed by using software (SPSS® 19.0 for Windows; IBM Corp., New York, NY; formerly SPSS Inc., Chicago, IL).

RESULTS

The IVIM MR images showed adequate imaging quality for imaging analysis in all 108 healthy participants. Figure 1 shows an example of ROI selection and the corresponding parametric maps derived from IVIM MRI in a 48-year-old female participant.

There was a significant inverse correlation between age and *D* or *f* value in both left (*D*: $p < 0.0001$, $r = -0.5035$; *f*: $p < 0.0001$, $r = -0.5265$) and right parotid glands (*D*: $p < 0.0001$, $r = -0.5700$; *f*: $p < 0.0001$, $r = -0.5690$), whereas no significant correlation was found between age and *D** values in both left (*D**: $p = 0.0688$, $r = -0.1758$) and right parotid glands (*D*: $p = 0.1209$, $r = -0.1503$). Detailed results about the correlation between the IVIM MRI parameters and the age are shown in Figure 2.

The parotid glands of the male participants demonstrated significantly higher mean *D*, *D** and *f* values than those of the female volunteers in both left (*D*: 1.0492 ± 0.0970 *vs* 0.9749 ± 0.1295, $p = 0.0041$; *D**: 20.5543 ± 1.3862 *vs* 18.0044 ± 2.0851, $p < 0.0001$; *f*: 0.2051 ± 00423 *vs* 0.1896 ± 0.0267, $p = 0.0468$) and right parotid glands (*D*: 1.0636 ± 0.0939 *vs* 0.9819 ± 0.1262, $p = 0.0014$; *D**: 20.3660 ± 1.4198 *vs* 17.8671 ± 2.0236, $p < 0.0001$; *f*: 0.2079 ± 0.0399 *vs* 0.1908 ± 0.0269, $p = 0.0208$). Effect of gender on the IVIM MRI parameters of bilateral parotid glands is shown in Table 1.

There were no significant differences on the *D*, *D** and *f* values between the left and right parotid glands (*D*: 0.9988 ± 0.1240 *vs* 1.0077 ± 0.1210, $p = 0.1534$; *D**: 18.8396 ± 2.2170 *vs* 18.6824 ± 2.1686, $p = 0.3226$; *f*: 0.1939 ± 0.0324 *vs* 0.1957 ± 0.0316, $p = 0.0700$). Meanwhile, there were no significant differences on the *D*, *D** and *f* values between the left and right parotid glands in the subgroup of either female or male participants (all $p > 0.05$). Effect of laterality on the IVIM MRI parameters of parotid glands is shown in Table 2. Conventional T_1 weighted and T_2 weighted MR images and the corresponding parametric maps derived from IVIM MRI in a 77-year-old female participant are shown in Figure 3.

Table 3 summarizes the interreader and intrareader agreement about the measurement of *D*, *f* and *D** values by using the corresponding ICCs and 95% confidence intervals. Excellent interreader and intrareader agreement about the measurements of the *D*, *f* and *D** values was achieved (interreader ICCs for *D*, *f* and *D**, 0.951, 0.877 and 0.822, respectively; intrareader ICCs for *D*, *f* and *D**, 0.968, 0.881 and 0.841, respectively).

DISCUSSION

Our study observed significant age-related changes on the *D* and *f* values of the parotid glands in healthy participants. As the age increased, the *D* and *f* values gradually decreased. However, no

Table 2. Effect of laterality on the intravoxel incoherent motion MRI parameters of parotid glands

Parameter	Female			Male		
	D	*D**	*f*	*D*	*D**	*f*
Left	0.9749 ± 0.1295	18.0044 ± 2.0851	0.1896 ± 0.0267	1.0492 ± 0.0970	20.5543 ± 1.3862	0.2051 ± 0.0423
Right	0.9819 ± 0.1262	17.8671 ± 2.0236	0.1908 ± 0.0269	1.0636 ± 0.0939	20.3660 ± 1.4198	0.2079 ± 0.0399
p-value	0.3473	0.5222	0.3365	0.2003	0.3646	0.0651

*D**, pseudodiffusion coefficient; *D*, tissue diffusivity; *f*, perfusion fraction.
Except *p*-values, data are expressed as mean ± standard deviation. The unit for *D* and *D** value is $\times 10^{-3}\,mm^2\,s^{-1}$.

Figure 3. Conventional axial T_1 weighted (a) and T_2 weighted images (b), an example of region of interest selection (c) and the corresponding parametric maps (d–f) derived from intravoxel incoherent motion (IVIM) MRI in a 77-year-old female participant. There was no significant difference on the IVIM-derived parameters between left and right parotid glands (D, 0.7154 *vs* 0.7251 × 10^{-3} mm^2 s^{-1}; D^*, 18.9502 *vs* 19.4549 × 10^{-3} mm^2 s^{-1}; f, 0.1714 *vs* 0.1732). Note that the IVIM-derived parameters of the parotid gland in this patient were lower than those in the patient showed in Figure 1.

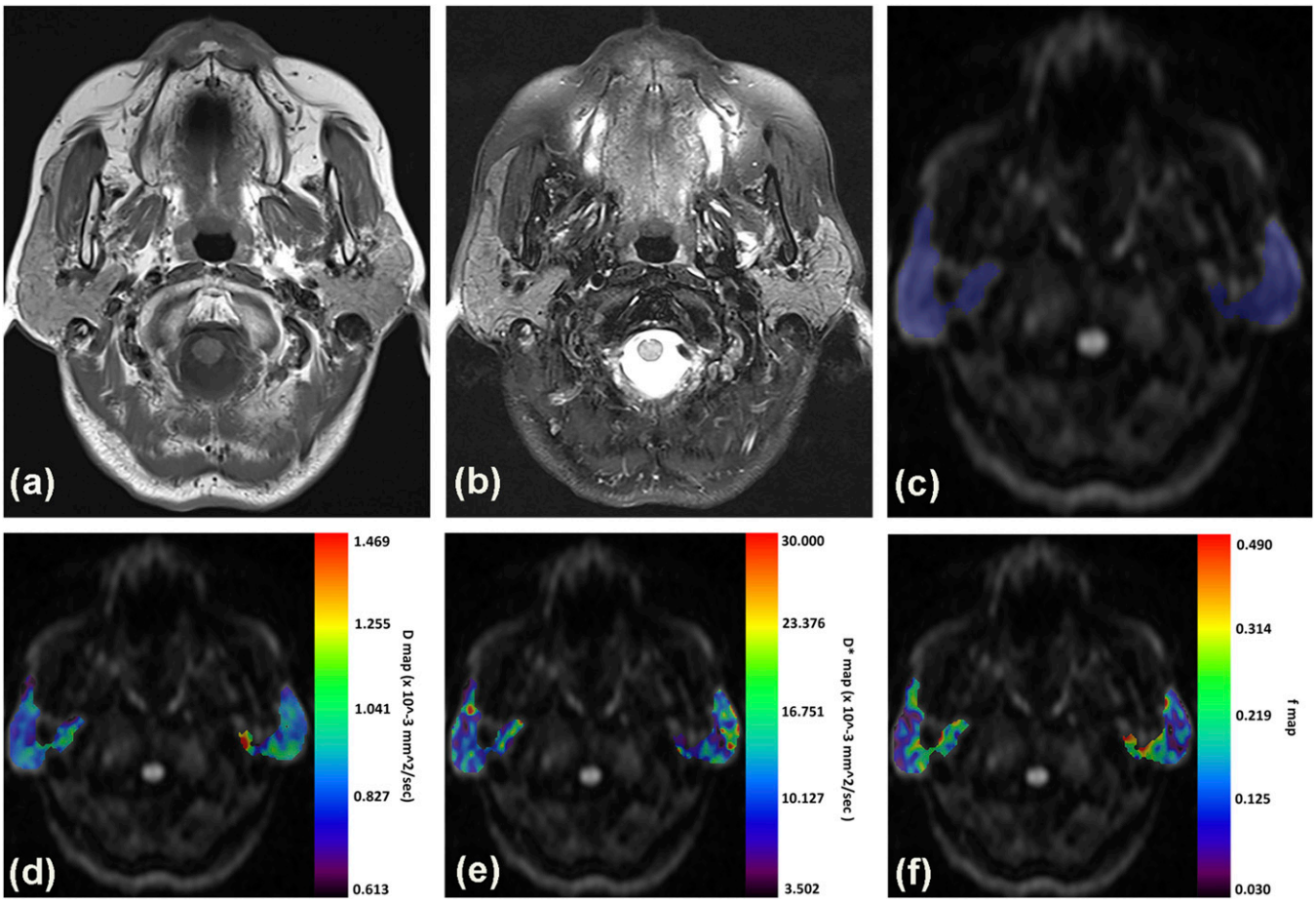

significant age-related changes were found for the D^* value. Meanwhile, our study revealed that the parotid glands of the male participants demonstrated significantly higher mean D, D^* and f values than those of the female participants. However, no significant difference was found for the IVIM MRI parameters between the left and right parotid glands. To the best of our knowledge, our study is the first one that investigates the effect of age, gender and laterality on the IVIM MRI measurements of parotid glands.

Previous studies[6,16,17] have shown the age-related changes of several imaging-related quantitative measurements of parotid glands, including T_1 intensity ratio, CT value and peak T_2 value. They found that the T_1 intensity ratio and peak T_2 value increased, and the CT value decreased with age, and they explained that an increasing fatty content replacement of the parenchyma of the parotid gland with age might be the potential reason.[6] We found clear age-related tendency for D and f values, and the possible mechanism that they proposed could also help to explain our finding. A previous study[11] proposed that prolonged T_2 of the tissue would lead to a lower calculated value of f, and then the fatty content replacement in the aged parotid glands would make the f value decreased. In addition, besides the fatty content, the parenchyma of the parotid gland could also

Table 3. Interreader and intrareader intraclass correlation coefficients (ICCs) for measurements of imaging parameters

Parameter	Interreader ICC	Intrareader ICC
D ($\times 10^{-3}$ mm^2 s^{-1})	0.951 (0.939–0.977)	0.968 (0.937–0.986)
f	0.877 (0.851–0.903)	0.881 (0.862–0.909)
D^* ($\times 10^{-3}$ mm^2 s^{-1})	0.822 (0.781–0.851)	0.841 (0.817–0.868)

Data in parentheses are the 95% confidence intervals.

partially be replaced by the fibrotic content, this fact could also make the D and f values decreased.[6] Therefore, it was not surprising that the f and D values would demonstrate inverse correlation with the age.

However, we did not find the similar inverse correlation between the D^* value and the age. We proposed that this fact might be due to the relatively worse repeatability of the measurement of D^* value.[18,19] Federau et al[18] ever found that D^* value was highly dependent on the cardiac cycle, the D^* value was significantly larger during systole than diastole, while D and f values did not vary significantly.[19] However, in our study, we did not perform echocardiography triggering during MR scan or some imaging correction during the imaging process. Therefore, the measurement of D^* value varied a lot and did not demonstrate similar inverse correlation as f and D values did.

Gender difference in parotid gland function has been observed in many other clinical studies.[7,8] Inoue et al[8] found that the males had higher unstimulated whole saliva flow rate than the females. Similarly, in our study, IVIM MRI measurements of the parotid glands of the males were significantly higher than those of the females. The difference in diffusion and perfusion characters is probably another form of parotid gland function variation between males and females. Further studies that correlate the parotid gland function with the diffusion or perfusion character would be significant for our hypothesis.

There was no significant difference on the IVIM MRI parameters between the left and right parotid glands and also in the subgroup analysis of either male or female participants. Therefore, the bilateral difference on the IVIM MRI parameters between the left and right parotid glands could be ignored when applying the IVIM MRI technique in the parotid gland disease. If unilateral parotid gland disease was suspected, the IVIM MRI parametric maps and corresponding quantitative measurements of the contralateral parotid gland could serve as reference for detecting lesions.

Previously, several researchers have used the IVIM MRI technique to evaluate the salivary gland disease.[12,13] Marzi et al[12] studied the temporal change of the IVIM-derived perfusion and diffusion parameters of the irradiated major salivary glands. Their study results provided new insights into the mechanisms of radiation injury to salivary glands. Besides that, considering that diffusion-weighted imaging has been used to study the parotid gland abnormality in Sjögren's syndrome, further studies that used IVIM imaging to demonstrate the diffusion and perfusion abnormality of the parotid glands in patients with Sjögren's syndrome would be very interesting.[20] In a word, IVIM imaging could serve as a promising imaging modality in the field of parotid gland disease. Then, based on our present study results, we think that age and gender factors must be taken into consideration in the interpretation of IVIM imaging parameters of parotid glands. The parameters adapted to age and gender may improve the study accuracy in future studies that use IVIM MRI to evaluate the parotid gland disease.

Our study had several limitations. First, IVIM MRI measurements could also be influenced by some involuntary motions, such as the cardiac cycle. However, we did not perform echocardiography triggering during MR scan or some imaging correction during the imaging process. This fact would affect the study result to a certain extent. Second, we did not correlate perfusion or diffusion parameters that derived from IVIM MRI with the parotid gland functional parameters, such as the unstimulated whole saliva flow rate. Further studies that correlate the IVIM MRI with the parotid gland function would be helpful for the application of IVIM MRI in evaluating various parotid gland diseases. Third, the sample size was relatively small. Further analyses with larger numbers of participants will be needed to validate our results.

In conclusion, our study performs age-, gender- and laterality-specific analyses of IVIM MRI parameters of the parotid gland in healthy participants. Our study results demonstrate that the IVIM MRI parameters are age and gender dependent but not laterality dependent. Our results indicate that the effect of age and gender need to be considered in future studies that use IVIM MRI to evaluate the parotid gland disease.

REFERENCES

1. Kato H, Kanematsu M, Watanabe H, Kajita K, Mizuta K, Aoki M, et al. Perfusion imaging of parotid gland tumours: usefulness of arterial spin labeling for differentiating Warthin's tumours. *Eur Radiol* 2015; **25**: 3247–54. doi: 10.1007/s00330-015-3755-7
2. Kato H, Kanematsu M, Watanabe H, Mizuta K, Aoki M. Salivary gland tumors of the parotid gland: CT and MR imaging findings with emphasis on intratumoral cystic components. *Neuroradiology* 2014; **56**: 789–95. doi: 10.1007/s00234-014-1386-3
3. Zhu L, Wang P, Yang J, Yu Q. Non-Hodgkin lymphoma involving the parotid gland: CT and MR imaging findings. *Dentomaxillofac Radiol* 2013; **42**: 20130046. doi: 10.1259/dmfr.20130046
4. Nabaa B, Takahashi K, Sasaki T, Okizaki A, Aburano T. Assessment of salivary gland dysfunction after radioiodine therapy for thyroid carcinoma using non-contrast-enhanced CT: the significance of changes in volume and attenuation of the glands. *AJNR Am J Neuroradiol* 2012; **33**: 1964–70. doi: 10.3174/ajnr.A3063
5. Sumi M, Takagi Y, Uetani M, Morikawa M, Hayashi K, Kabasawa H, et al. Diffusion-weighted echoplanar MR imaging of the salivary glands. *AJR Am J Roentgenol* 2002; **178**: 959–65. doi: 10.2214/ajr.178.4.1780959
6. Saito N, Sakai O, Bauer CM, Norbash AM, Jara H. Age-related relaxo-volumetric quantitative magnetic resonance imaging of the major salivary glands. *J Comput Assist Tomogr* 2013; **37**: 272–8. doi: 10.1097/RCT.0b013e31827b4729
7. Chang HC, Juan CJ, Chiu HC, Cheng CC, Chiu SC, Liu YJ, et al. Effects of gender, age, and body mass index on fat contents and apparent diffusion coefficients in healthy parotid glands: an MRI evaluation. *Eur Radiol* 2014; **24**: 2069–76. doi: 10.1007/s00330-014-3265-z

8. Inoue H, Ono K, Masuda W, Morimoto Y, Tanaka T, Yokota M, et al. Gender difference in unstimulated whole saliva flow rate and salivary gland sizes. *Arch Oral Biol* 2006; **51**: 1055–60. doi: 10.1016/j.archoralbio.2006.06.010
9. Le Bihan D, Breton E, Lallemand D, Aubin ML, Vignaud J, Laval-Jeantet M. Separation of diffusion and perfusion in intravoxel incoherent motion MR imaging. *Radiology* 1988; **168**: 497–505. doi: 10.1148/radiology.168.2.3393671
10. Jia QJ, Zhang SX, Chen WB, Liang L, Zhou ZG, Qiu QH, et al. Initial experience of correlating parameters of intravoxel incoherent motion and dynamic contrast-enhanced magnetic resonance imaging at 3.0 T in nasopharyngeal carcinoma. *Eur Radiol* 2014; **24**: 3076–87. doi: 10.1007/s00330-014-3343-2
11. Sumi M, Van Cauteren M, Sumi T, Obara M, Ichikawa Y, Nakamura T. Salivary gland tumors: use of intravoxel incoherent motion MR imaging for assessment of diffusion and perfusion for the differentiation of benign from malignant tumors. *Radiology* 2012; **263**: 770–7. doi: 10.1148/radiol.12111248
12. Marzi S, Forina C, Marucci L, Giovinazzo G, Giordano C, Piludu F, et al. Early radiation-induced changes evaluated by intravoxel incoherent motion in the major salivary glands. *J Magn Reson Imaging* 2015; **41**: 974–82. doi: 10.1002/jmri.24626
13. Zhang L, Murata Y, Ishida R, Ohashi I, Yoshimura R, Shibuya H. Functional evaluation with intravoxel incoherent motion echo-planar MRI in irradiated salivary glands: a correlative study with salivary gland scintigraphy. *J Magn Reson Imaging* 2001; **14**: 223–9. doi: 10.1002/jmri.1177
14. Zhang YD, Wang Q, Wu CJ, Wang XN, Zhang J, Liu H, et al. The histogram analysis of diffusion-weighted intravoxel incoherent motion (IVIM) imaging for differentiating the gleason grade of prostate cancer. *Eur Radiol* 2015; **25**: 994–1004. doi: 10.1007/s00330-014-3511-4
15. Kim DY, Kim HS, Goh MJ, Choi CG, Kim SJ. Utility of intravoxel incoherent motion MR imaging for distinguishing recurrent metastatic tumor from treatment effect following gamma knife radiosurgery: initial experience. *AJNR Am J Neuroradiol* 2014; **35**: 2082–90. doi: 10.3174/ajnr.A3995
16. Sumi M, Izumi M, Yonetsu K, Nakamura T. Sublingual gland: MR features of normal and diseased states. *AJR Am J Roentgenol* 1999; **172**: 717–22. doi: 10.2214/ajr.172.3.10063867
17. Mahne A, El-Haddad G, Alavi A, Houseni M, Moonis G, Mong A, et al. Assessment of age-related morphological and functional changes of selected structures of the head and neck by computed tomography, magnetic resonance imaging, and positron emission tomography. *Semin Nucl Med* 2007; **37**: 88–102. doi: 10.1053/j.semnuclmed.2006.10.003
18. Federau C, Hagmann P, Maeder P, Müller M, Meuli R, Stuber M, et al. Dependence of brain intravoxel incoherent motion perfusion parameters on the cardiac cycle. *PLoS One* 2013; **8**: e72856. doi: 10.1371/journal.pone.0072856
19. Lee Y, Lee SS, Kim N, Kim E, Kim YJ, Yun SC, et al. Intravoxel incoherent motion diffusion-weighted MR imaging of the liver: effect of triggering methods on regional variability and measurement repeatability of quantitative parameters. *Radiology* 2015; **274**: 405–15. doi: 10.1148/radiol.14140759
20. Ding C, Xing X, Guo Q, Liu D, Guo Y, Cui H. Diffusion-weighted MRI findings in Sjögren's syndrome: a preliminary study. *Acta Radiol* 2015. [Epub ahead of print].